Vegetation and fire anomalies during the last ~70 ka in the Ili Basin, Central Asia

Yunfa Miao [a, b]*, Yougui Song [b, c]*, Yue Li [b, d], Shengli Yang [e], Yun Li [b]

a. Key Laboratory of Desert and Desertification, Northwest Institute of Eco-Environment and Resources, Chinese Academy of Sciences, Lanzhou 730000, China

b. State Key Laboratory of Loess and Quaternary Geology, Institute of Earth Environment, Chinese Academy of Sciences, Xi'an 710061, China

c. Research Center for Ecology and Environment of Central Asia, Chinese Academy of Sciences, Urumqi, 830011, China

d. College of Resources and Environment, University of Chinese Academy of Sciences, Beijing, 100049 China

e. Key Laboratory of Western China's Environmental Systems（Ministry of Education), College of Earth and Environmental Sciences, Lanzhou University, Lanzhou, 730000, China

Corresponding author: miaoyunfa@lzb.ac.cn; ygsong@loess.llqg.ac.cn

Abstract: Records of vegetation characteristics and fire activity obtained from the same profile can offer an opportunity to better understand paleoclimatic and paleoecological changes and their underlying driving forces. Here, we present sporopollen (spores and pollen) and microcharcoal data collected together from the wind-blown loess Nileke (NLK) section, representing the past ~70 thousand years (ka) in the Ili Basin (Northwest China), Central Asia. Results reveal that the temperate woody taxa (e.g., Cupressaceae) remained at high levels before 36 ka, while the total microcharcoal concentrations (MC) were relatively low. After 36 ka, the herbaceous taxa (e.g., *Artemisia*, Chenopodiaceae) abruptly replaced the woody taxa and the MC increased. This vegetation degeneration at 36 ka is notable because no equivalent changes have been identified anywhere else across Eurasia. Another interesting observation is that the vegetation degeneration immediately followed a period characterized by an increased number of larger microcharcoal particles, in contrast to the smaller sizes occurring between 47.5 and 36 ka. This pattern can be explained in terms of (1) a special, localized environment event caused by the particular special taphonomic effects or sedimentary processes unrelated to the fire strength/frequency; or (2) an

ecological event driven by human activities, such as burning the local vegetation near the NLK site. The latter case is argued to be more likely. Future analysis of first-hand archeological sites in this area will be an important step in checking this hypothesis.

Keywords: Vegetation; Fire; Anomaly; Human activities; Last glacial period

1. Introduction

The climate, vegetation, fire and human activities, as well as the relationships among them during the late Quaternary, especially the last glacial period, provide basic insights by which to understand the future (e, g., Behling and Safford, 2010; Cheng et al., 2012; Li et al., 2013; Hubau et al., 2015; Varela et al., 2015). High-resolution stalagmite (Wang et al., 2001; Cheng et al., 2012), ice core (Thompson et al., 1997; Petit et al., 1999; Augustin et al., 2004) and loess (e.g., Chen et al., 1997; Hao et al., 2012; Sun et al., 2012; Rao et al., 2013) analysis has yielded many paleoclimate records. These are characterized by a series of strong fluctuations, named cold Heinrich or warm Dansgaard-Oeschger events, as well as a warm middle Holocene (e.g., Bond et al., 1997). However, as the most sensitive organic proxies for terrestrial climate change, a limited number of complete vegetation records have been obtained to show how the terrestrial ecological landscape responded to the climate change (e.g., Guiot et al., 1993; Allen et al., 1999; Jiang et al., 2011; Nigst et al., 2014). These have revealed that the vegetation changes are largely a response to natural climate change, with no strong evidence to suggest that humans have significantly disturbed/changed the vegetation/ecology until the late Holocene (e.g., Nigst et al., 2014). Additionally, fire is another sensitive proxy used for reconstructing climate and ecology (e.g., Filion, 1984; Bird and Cali, 1998; Bowman et al., 2009). Besides climate and ecology, records of vegetation and fire together are also unique indicators of human activities, owing to the impact of human activities such as vegetation cutting and burning (e.g., Patterson et al., 1987; Whitlock and Larsen, 2002; Huang et al., 2006; Aranbarri et al., 2014; Miao et al., 2016a, 2017; Sirocko et al., 2016); however, most relevant studies have been limited to the late Holocene, especially at or near archeological sites (Miao et al., 2017), although anthropogenic fire has been evidenced earlier than 1000 ka ago (e.g., Clark and Harris, 1985; Gowlett and Wrangham, 2013). In fact, the last glacial period is considered as a key period of modern human's migration: the human migration from

Africa started at ~200 ka ago and spread into Eurasia (Templeton, 2002; Sun et al., 2012), so studies of vegetation and fire within the same profile (section or core) are helpful in understanding the vegetation, fire and climate change, as well as human activities (e.g., Zhao et al., 2010; Wang et al., 2013; Miao et al., 2016a; 2017).

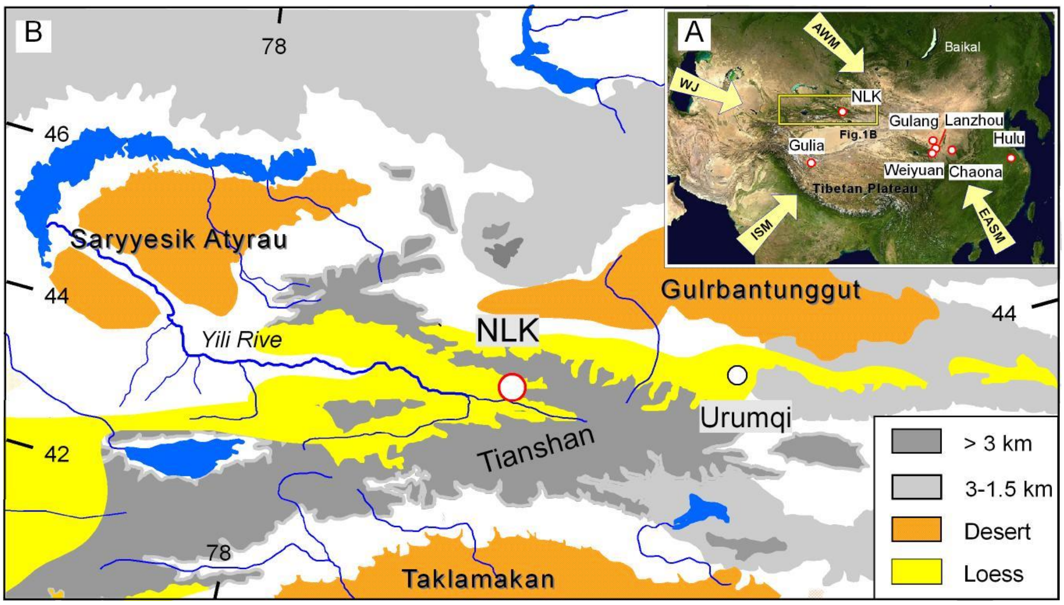

Figure 1. A. Asian morphological map with climate systems showing the NLK section location and climatic proxy sites covering the past 70 ka. These sites include the Gulia glacial core (Thompson et al., 1997), Gulang wind-blown sediments (Sun et al., 2012), Chaona (Wang et al., 2016), Hulu stalagmite oxygen isotope records (Wang et al., 2001), Weiyuan summer precipitation reconstruction (Rao et al., 2013) and Lanzhou pollen analysis (Jiang et al., 2011). B. A morphological map showing the location of the NLK section in this study. ASM: Asian summer monsoon; ISM: Indian summer monsoon; WJ: Westerly jet; AWM: Asian winter monsoon.

Central Asia is dominated by a dry climate (Figure 1A), which is very sensitive to any climate changes (fluctuations or anomalies) and human activities. In this study, we firstly present pollen and microcharcoal results from a wind-blown loess sediment section (Figure 1B) to reveal how vegetation and fire activity have changed during the past 70 ka; we then analyze the mechanisms underlying these changes.

2. Materials and methods

2. 1 Lithostratigraphy and chronology

The Ili Basin is surrounded by the Tianshan orogenic belt in east Central Asia, with gentle topography to the west. The basin opens to the west and funnels winds and cyclonic disturbances, often associated with prevailing westerly winds (Ye, 2001). The Ili Basin has a temperate, continental, arid climate with a mean annual temperature that varies from 2.6 ℃ at 1850 m to 10.4 ℃ at 660 m; the mean annual precipitation varies correspondingly from 512 to 257 mm (Ye et al., 1997). The surface soils are a sierozem (aridosols) with widely distributed desert steppe vegetation. The vegetation coverage is <50%, mainly comprising *Artemisia* spp. and Chenopodiaceae spp. There are no obvious accumulations of organic matter in the surface horizon of the modern soil.

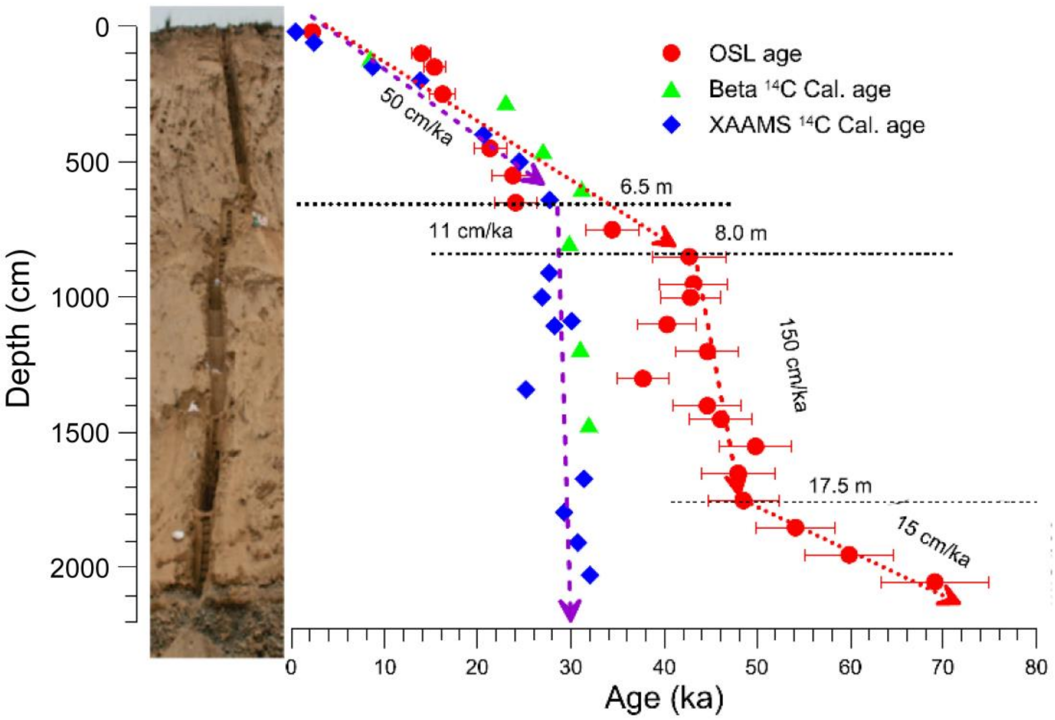

Figure 2. Stratigraphy and dating for the NLK Section. Radiocarbon ages (Beta and XAAMS) appear to saturate below a depth of 6.5 m at ca. 30 cal ka BP (purple dashed line), while the OSL ages continue to increase with depth. The OSL ages are used as an age-depth model (for more details see Song et al. 2015).

To the west of the Ili Basin are the vast central Asian Gobi Deserts, such as Saryesik-Atyrau Desert (Figure 1B), the probable source of dust for Late Pleistocene loess deposits. The loess deposits are widely distributed across the piedmont of the Tianshan Mountains, river terraces and desert margins. The loess thickness ranges from several meters to approximately two hundred meters, and there are two primary depocenters: around Sangongxiang in the northwest and Xinyuan in the east Ili basin (Song et al., 2014). Most of the loess appears to have been deposited since the last interglacial period (ca. 130 ka ago; Ye, 2001; Song et al., 2010; 2014; Li et al., 2016).

The NLK section (83.25 °E, 43.76 °N, 1253 m a. s. l) is located on the second terrace of the Kashi River, a branch of the Ili River, in the east of the Ili Basin (Figure 1B). The loess sequence is 20.5 m thick, largely homogeneous in appearance with two diffuse paleosols at depths of 5-7.5 m and 15.5-18.5 m (Figure 2) (Song et al., 2015). The loess sequence rests conformably on fluvial sand and gravels. The contact between the loess and fluvial sediment is abrupt, with no obvious lag, erosion or pedogenesis. The loess is composed of 70%-84% silt and 3%-17% very fine sand (63-100 mm), with the remaining fraction being clay. A high-resolution quartz optically stimulated luminescence (OSL) chronology has already been established (Yang et al., 2014; Song et al., 2015). Based on these OSL ages, two intervals of higher mass accumulation rate occurred at 49-43 ka and 24-14 ka ago (Song et al., 2015).

2.2 Pollen and charcoal collection

A total of 104 samples of 49-56 g weight were taken at 20 cm intervals from the NLK section for palynological analysis. The samples were treated with standard palynological methods: acid digestion (treatment with 10% HCl and 40% HF acid to remove carbonates and silicates, respectively) and fine sieving to enrich the spores and pollen grains. The prepared specimens were mounted in glycerol for identification. All samples were studied at the Cold and Arid Regions Environmental and Engineering Research Institute (CAREERI), Chinese Academy of Sciences (CAS), by comparison with official published pollen plates and modern pollen references. Each pollen sample was counted under a light microscope at 400× magnification in regularly spaced traverses. More than 150 spores and pollen grains were counted within each sample. A known number of *Lycopodium clavatum* spores (batch # 27600) were initially added to each sample for calculation of pollen and microcharcoal concentrations (Maher, 1981).

The concentration of pollen or microcharcoals can be calculated according to the following formula: $C=N_x/L_x \times 27600/W_x$

C: concentration; *N*: identified number of charcoals; *L*: number of *Lycopodium clavatum*; *W*: sample dry weight; x: sample number; 27600: grain numbers of *Lycopodium clavatum* per pill.

For the microcharcoal identification, four particle size units were defined as follows: <30 μm, 30-50 μm, 50-100 μm and >100 μm (Miao et al., 2016a), then the total microcharcoal concentrations (MC) were obtained by summing over all sizes and using the above formula. As the residual matter from the incomplete burning of vegetation, charcoals are usually characterized either by spherical bodies without structure or by particles with some original plant structures preserved.

3. Results and analysis

In the pollen assemblages, dominant palynomorphs originated mainly from the herbaceous taxa such as Chenopodiacaee, *Artemisia*, Ranunculaceae, Asteraceae and Rosaceae. Woody taxa were Cupressaceae, *Pinus*, *Betula*, Ulmaceae and Tamaricaeae; the other temperate taxa with low percentages were *Quercus*, *Picea*, *Cedrus* and *Broussanetia* etc.

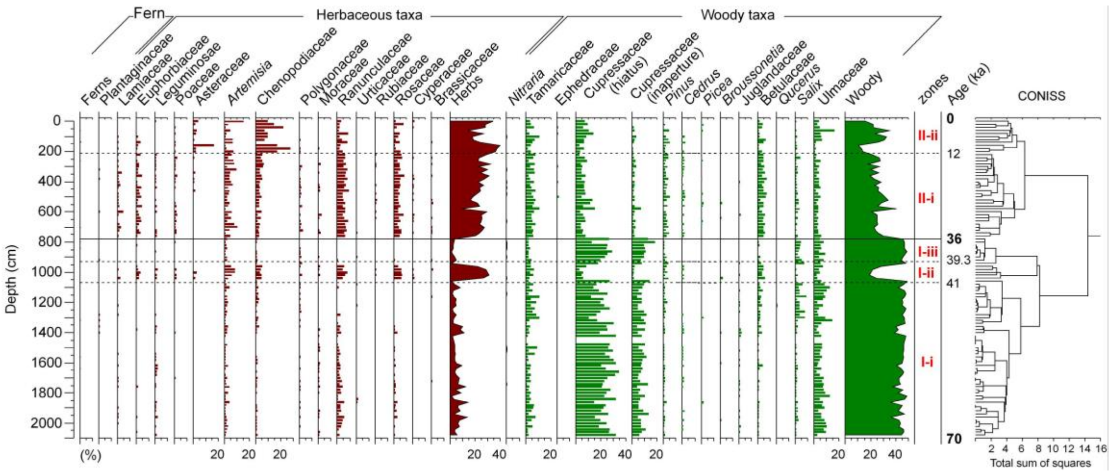

Figure 3. Pollen percentage diagram for the NLK section, Ili Basin.

The pollen diagram was divided into two pollen assemblage zones based on variations in the percentages according to stratigraphically-constrained cluster analysis (CONISS) carried out using Tilia software (E. Grimm of Illinois State Museum, Springfield, Illinois, USA) (Figure 3) and concentrations of the dominant taxa, from the older to the younger samples. The two zones are as follows.

Zone I (2080-780 cm; 70-36 ka ago): the assemblages were characterized by high percentages of Cupressaceae (hiatus) (ca. 5.2%-68.7%, with an average of 42.4%) and Cupressaceae (inaperture) (ca. 1.4%-34.7%, average 14.0%), Ulmaceae (ca. 2.8%-26.1%, average 11.3%) and, Tamaricaceae (ca. 1.9%-20.9%, average 7.3%). In the herbaceous taxa, only *Artemisia* (ca. 0-14.8%, average 3.3%), Rannuculaceae (ca. 0-14.2%, average 3.0%) and Chenopodiacae (ca. 0-8%, average 1.8%) were dominant, and were present at much lower abundances relative to the woody taxa. In more detail, three subzones were identified according to the assemblages: I-i, I-ii and I-iii with divisions at 1070 and 930 cm, corresponding to ages of 41 ka and 39.3 ka. The subzones I-i and I-iii were both characterized by high Cupressaceae, whereas subzone I-ii was dominated by herbaceous taxa.

In the pollen concentrations, the same zones were also identified at a depth of 780 cm. The woody taxa were dominant below this boundary, and those such as Cupressaceae (hiatus and inaperture), Ulmaceae and Tamaricaceae reached counts of around 1000 grains/g, 200 grains/g and 100 gains/g, respectively. Others such as *Pinus*, Juglandaceae, *Betula* and *Salix* were also common. By contrast, all herbaceous taxa were very low (Figure 4). We also added the boundary at a depth of 780 cm to divide the MC assemblages. Below the boundary, the fluctuations in all different sizes and shapes were stronger, especially in Zones I-ii and I-iii (Figure 5).

Zone II (780-0 cm; 36-0 ka ago): the woody taxa were extensively replaced by herbaceous taxa, of which Cupressaceae (hiatus) (ca. 3.5%-51.0%, average 12.1%) and Cupressaceae (inaperture) (ca. 0-24.5%, average 2.9%), Tamaricaceae (ca. 1.5%-19.4%, average 8.9%) and Ulmaceae (ca. 0.5%-27.9%, average 5.6%) were dominant; *Betula* and *Pinus* increased slightly (ca. 0-12.6%, average 6.4% and ca. 0-8.6%, average 2.3%, respectively). In the herbaceous taxa, *Artemisia* (ca. 0.9-24.1%, average 7.1%), Chenopodiaceae (ca. 0-48.2%, average 9.0%), Rosaceae (ca. 0-15.0%, average 8.6%) and Rannuculaceae (ca. 0-14.2%, average 3.0%) increased obviously, and the rest remained broadly stable. In more detail, two sub-horizons were identified: II-i and II-ii, divided based on the Asteraceae and Chenopodiaceae increase at 210 cm, correlated to an age of 12 ka (Figure 3).

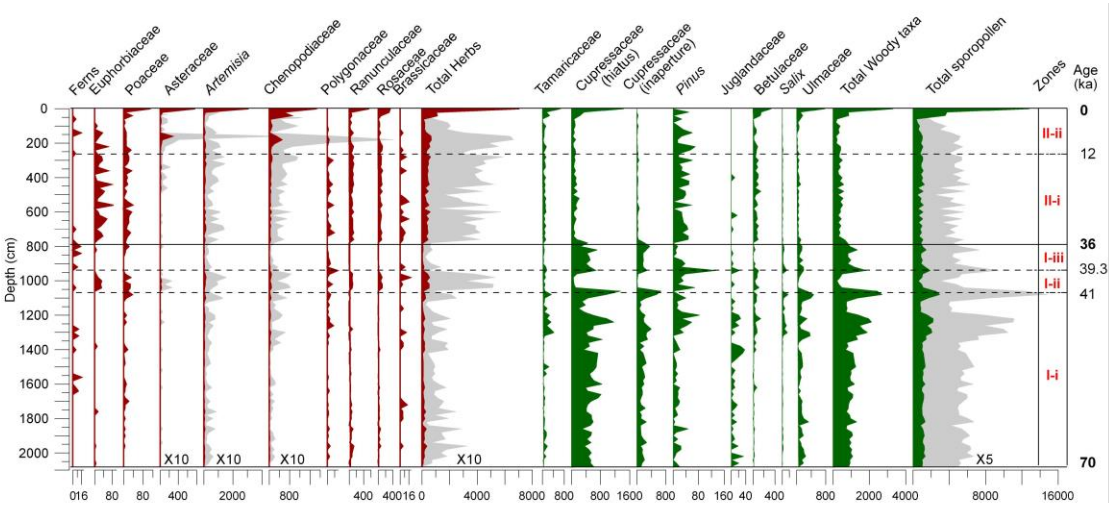

Figure 4. Pollen concentration diagram for the NLK section, Ili Basin, China (unit: grains/g; zone divisions follow Figure 3).

The pollen concentrations in Zone II show that the woody Cupressaceae (hiatus and inaperture), Ulmaceae, Juglandaceae and Tamaricaceae obviously decreased while the herbaceous taxa such as *Artemisia*, Chenopodiaceae, Poaceae, Ranuculaceae and Rosaceae increased. At the sub-boundary of II-i and II-ii, Asteraceae, *Artemisia* and Chenopodiaceae increased strongly (Figure 4). For the MC, all different shapes and sizes remained at generally stable and relatively low values in Zone II-i whereas in Zone II-ii the concentrations in all samples clearly started to increase, especially in the uppermost layers (Figure 5).

In summary, there are clear divisions at a depth of 780 cm, corresponding to an age of 36 ka. Prior to this change, there was a high percentage of woody taxa, but subsequently the herbaceous taxa became more dominant, especially after 12 ka. The assemblages of pollen concentrations and MC can also be divided into two periods, with a transition at 36 ka.

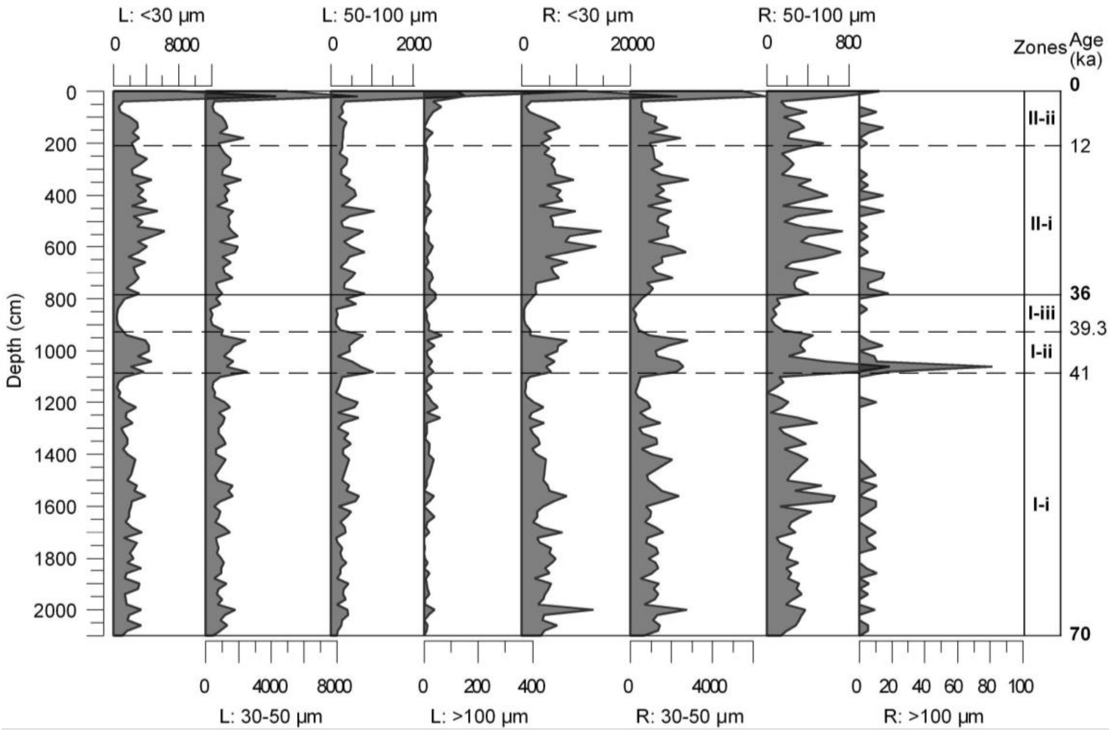

Figure 5. The MC records for different sizes and shapes in the NLK section (unit: grains/g; L: elongated shapes; R: rounder shapes; zone divisions follow Figure 3).

4. Discussion

The modern climate in Central Asia is controlled by the East Asian summer monsoon, Indian summer monsoon, Asian winter monsoon and Westerlies (Figure 1A). In the Ili Basin, meteorological records indicate that strong surface winds from the west, northwest and southwest which occur frequently from April to July play the dominant role in the transportation of dust, suggesting that the wind-blown sediments in the NLK section are driven by the Westerlies. Therefore, the grain size of the sediments can be regarded as a basic proxy for the intensification of the Westerlies (Li et al., 2015; Li et al., 2016). Furthermore, the Ili Basin is surrounded by the Tianshan Mountains to the south, east and north (with elevations exceeding 3-4 km) but low elevations (~800-1600 m a. s. l) to the west. Consequently, most of the precipitation reaching the basin will have been transported by the Westerlies during the last glacial period. Here, we try firstly to estimate changes in the vegetation and fire characteristics in the Ili Basin; secondly, to discuss the overall climate change across Eurasia over the past 70 ka; and finally, to provide some speculation regarding the observed differences.

4.1 Vegetation and fire anomalies at NLK

The pollen dataset can be regarded as a reliable proxy for investigating the vegetation change in the study area. In the NLK section, during 70-36 ka, the pollen assemblages show a relatively woody taxa-dominated landscape: during this time, the woody taxa reached their highest levels of the whole section (Figure 6). After 36 ka, the vegetation deteriorated markedly, as evidenced by the rapid disappearance of woody taxa following strong fluctuations during 41-36 ka. This was especially notable for Cupressaceae. In more detail, no obvious fluctuations were noted during these two periods except for during the interval between 41 and 36 ka. The pollen concentrations also followed a similarly stable trend except for the anomalies between 41 and 36 ka. Overall, the most obvious vegetation change according to the pollen data was at around 36 ka ago, as indicated by the sharp decrease of woody taxa in the vegetation assemblages. No similar vegetation transition has been observed in Eurasia (e.g., Guiot et al., 1993; Allen et al., 1999; Jiang et al., 2011).

Charcoal particles remaining following combustion are entrained in the smoke and then carried by the wind. Following deposition, they remain as a direct proxy of fire activity. On the Loess Plateau, smaller charcoal particles can be easily transported over long distances by the wind, but the larger particles tend to travel only a short distance (Huang et al., 2006). Therefore, the charcoal particle size can be related to its distance from the fire (Patterson et al., 1987; Clark, 1988; Luo et al., 2001; Miao et al., 2016a; 2017), with smaller particles likely to have been transported further from the fire (Clark, 1988). Moreover, a rounder shape (long axis to short axis ratio <2.5) is more likely related to forest fires while elongated particles (long axis to short axis ratio >2.5) are more indicative of grass fires (Umbanhowar and Mcgrath, 1998; Crawford and Belcher, 2014). The charcoal assemblages in the Ili Basin show a relatively low fire frequency/severity at regional and local scales, in forest and grass, before 36 ka; activities then increased gradually after 36 ka (Figures 6, 7). Superimposed on this general trend is the first notable anomaly, which occurred at 47.5-36 ka and was characterized by a high frequency of local grass and forest fires. Another similar anomaly occurred at the top of the profile (less than 6 ka ago) in the layer with the highest levels of regional and local grass fires as well as the highest regional forest fires (Figure 5).

In summary, the climate in the Ili Basin abruptly became arid at 36 ka ago, according to pollen data, while an unexpected strengthening in local fire activity occurred during 47.5-36 ka according to the microcharcoal data. Both vegetation and fire changes are different to those of the grain-size and clay mineral analysis from the same section (Figure 8).

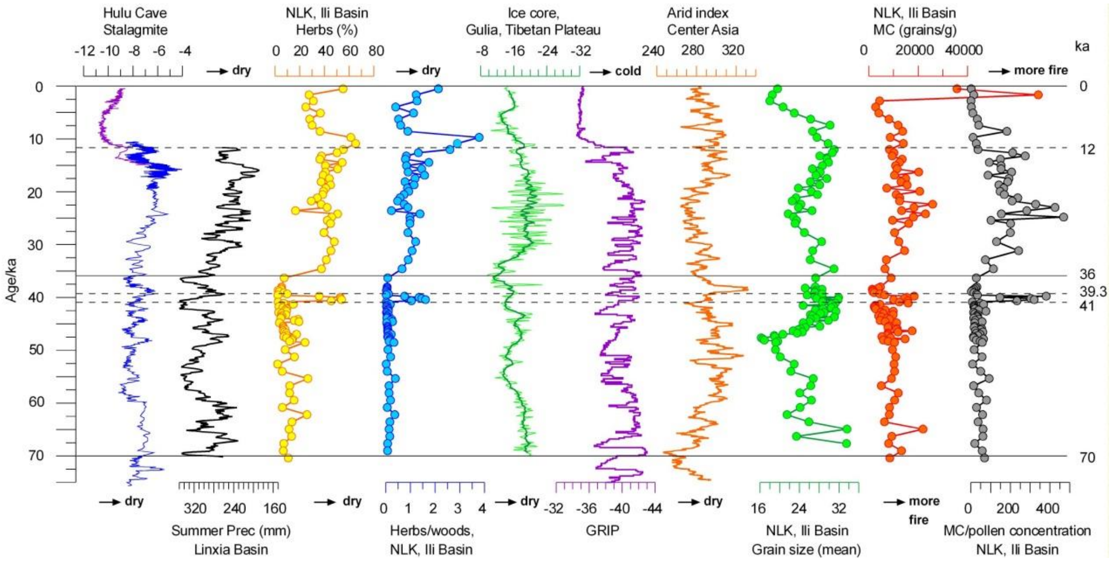

Figure 6. Comparison of climate proxies across the Northern Hemisphere and NLK section. These are the Hulu cave, Nanjing (Wang et al., 2001); summer precipitation reconstruction in the Linxia Basin (Rao et al., 2013); ice core, Gulia, Tibetan Plateau (Thompson et al., 1997); NGRIP (Andersen et al., 2004); and aridity index in central Asia (Li et al., 2013). Divisions follow Fig. 3.

4.2 Driving forces

Here, the global/regional climate background as well as its influence on the Central Asian vegetation and fire will be discussed first, followed by the potential influences of specific factors, such as taphonomic effects, sedimentary processes and human activities.

4.2.1 Global climate and fire background

Here, multiple proxies from terrestrial and marine sources have revealed the basic patterns of climate change during the last glacial period, characterized by abrupt, millennial-scale cold events (Petit et al., 1999; Wang et al., 2001; Augustin et al., 2004; Cheng et al., 2012) (Figure 6). These climate fluctuations are particularly pronounced in records of the East Asian monsoon system (Porter and An, 1995; Guo et al., 1996; Thompson et al., 1997; Wang et al., 2001; Sun et al., 2012).

The Greenland NGRIP ice core (Andersen et al., 2004) indicates that temperature variations in the high latitudes of the Northern Hemisphere have been characterized by high-frequency fluctuations over the past 70 ka, with the most obvious change occurring at around 12 ka ago but with no significant anomaly at 36 ka ago. At the same time, high-resolution summer precipitation variations in the western Chinese Loess Plateau were found to contain similar anomalies (Rao et al., 2013), yet with no obvious precipitation change at ca. 36 ka, despite their proximity to the Lanzhou loess sediments, where the shrubs and herbs reached the highest abundances after ca.40 ka owning to the strengthened westerlies bringing increased moisture to Northwest China (Jiang et al., 2011). Besides the temperature/precipitation changes, the levels of greenhouse gases, e.g., CH_4 (Blunier and Brook, 2001) and CO_2 (Ahn and Brook, 2008) during this period remained within the bounds of normal fluctuations. So, large-scale climate change across Eurasia cannot be the primary factor explaining the vegetation anomalies at ~36 ka ago and fire anomalies at 47-36.5 ka ago in the Ili Basin.

According to a contemporaneous fire study, the macroscopic charcoals from Eifel (Germany), central Europe reveal frequent drought stress and frequent forest fires during 49–36.5 ka, which appeared even stronger than those during 6-0 ka. The former is explained as a result of natural fires, and the latter is linked to the widespread alteration of the early Holocene forests by humans, as the charcoals contain elements from cereal and cattle farming (Figure 9) (Sirocko et al., 2016). Regardless of the underlying causes of these changes in Europe, the two periods of fire anomalies correlated well with the results from the NLK section (Figure 9).

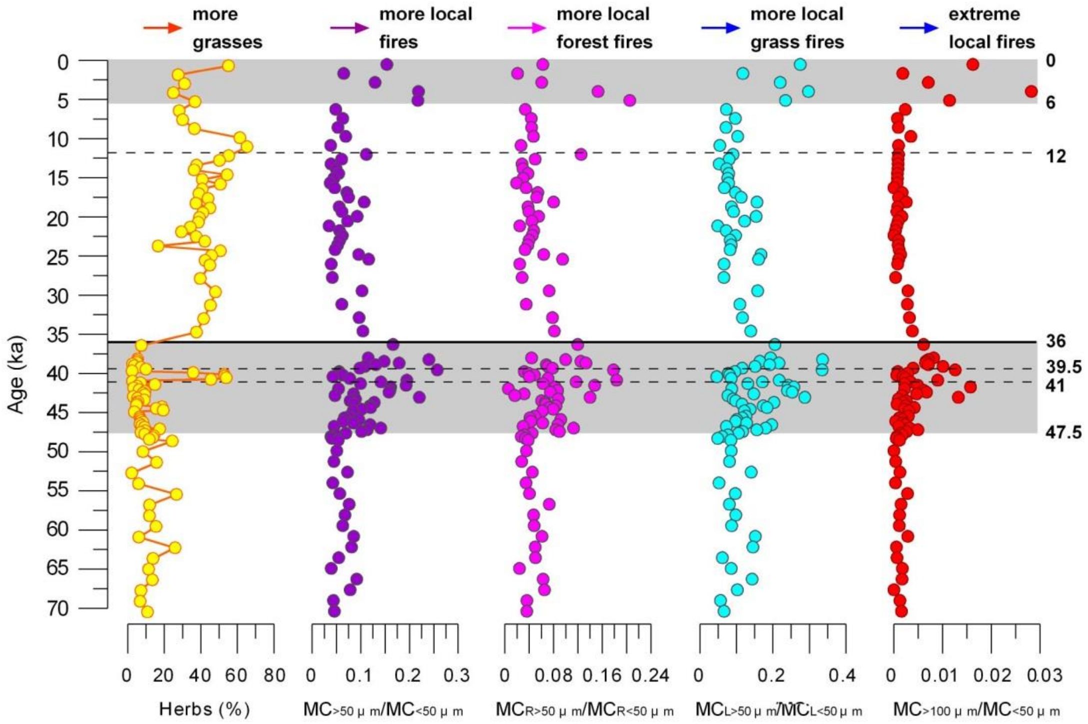

Figure 7. Vegetation versus fire anomalies identified in the NLK section during 47.5-36 ka. Gray rectangles show periods of intensified local fire activity during 47.5-36 and 6-0 ka, which cannot easily be explained as the result of the climate change.

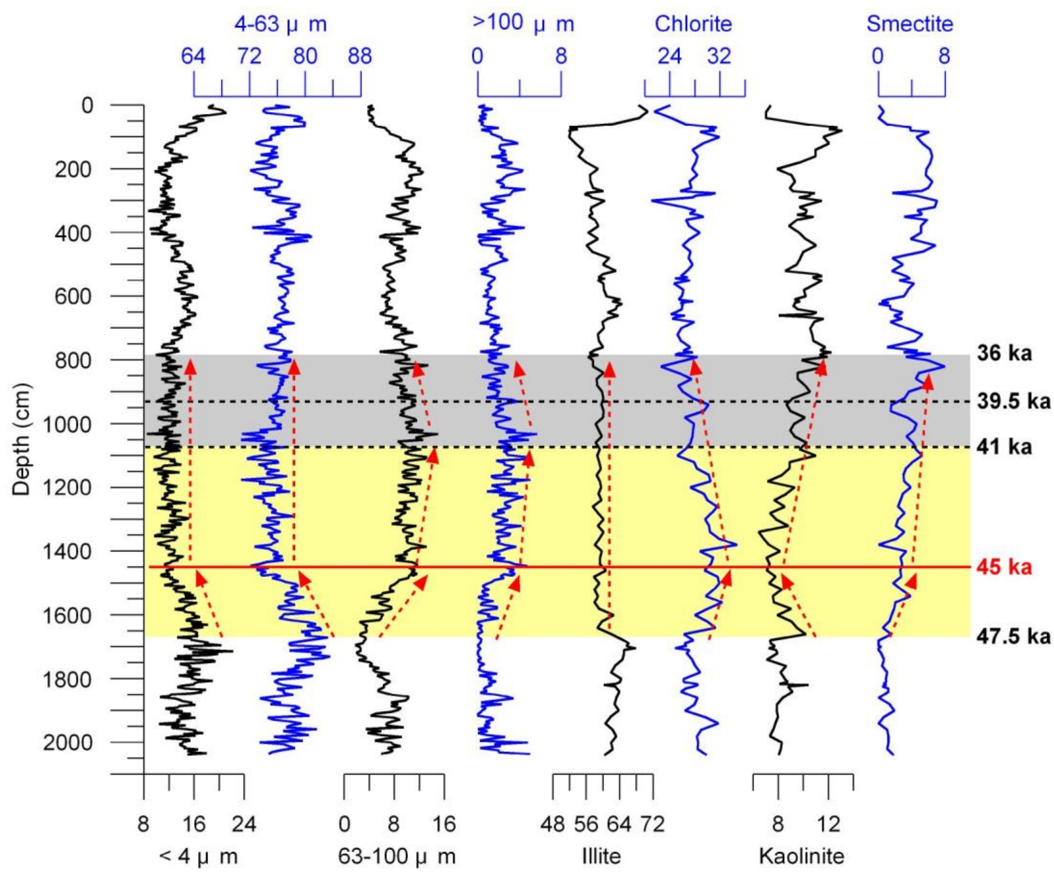

Figure 8. Grain-size distributions (<4 μm, 4-63 μm, 63-100 μm, and >100 μm, respectively) (Yang et al., 2014) and mineralogy in percentage weight of the main clay fraction (Illite, Chlorite, Kaolinite, and Smectitie)(Li et al., 2017) from the NLK section vs. depth. The gray and yellow shaded areas with ages indicate the vegetation and fire anomalies corresponding to Figures 3 and 7, respectively. The dashed red arrows show the trends, and the heavy red line indicates the obvious turning point of these trends at ~45 ka.

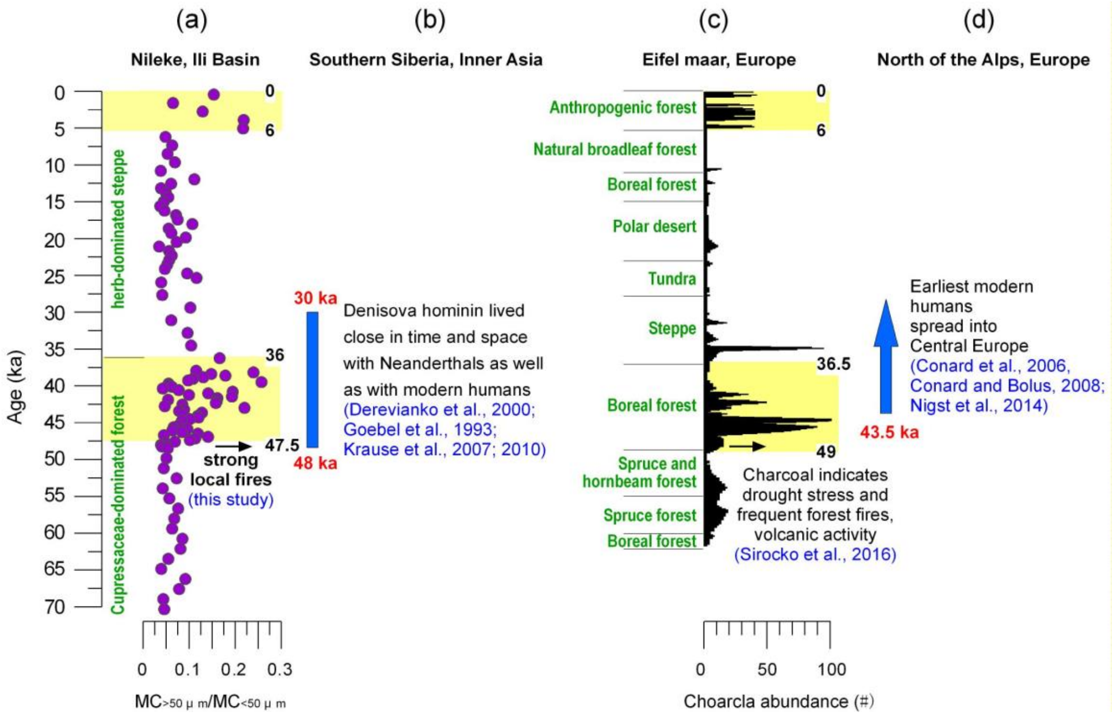

Figure 9. Correlations of (a) fire anomalies in the NLK section, Central Asia; (b) Denisova hominin periods, Central Asia; (c) fire anomalies in Eifel, Europe, and (d) modern humans beginning to colonize Europe. Both vegetation assemblages are according to the pollen data. Yellow rectangles indicate their own individual zones mentioned in this study based on the pollen assemblages.

4.2.2 Taphonomic effect

Although the climate usually plays a key role in vegetation and fire changes, the taphonomic process can, theoretically, disturb the paleoclimatic records and interpretation by oxidizing the pollen and microcharcoals during/after their burial. If oxidization does occur, some thin-walled pollen grains and small microcharcoals would disappear first and thus influence the pollen assemblages and fire interpretation, leading to erroneous paleoclimate/paleoecology inferences. Fortunately, this process does not have a significant impact. Firstly, pollen have a hard coat (wall) made of sporopollen, which is very difficult to oxidize. For example, the pollen of Cupressaceae are common in the Holocene (Chen et al., 2006) or even in some Quaternary aeolian sediments (Wu et al., 2007) in Central Asia, despite having a very thin wall. Here, high percentages of Cupressaceae pollen at the bottom of the section may indicate that the oxidization during/after burial has not influenced the pollen assemblages at all (Figures 3 and 4). Secondly, (micro-)

charcoal is a lightweight, black residue, consisting of carbon and any remaining ash, obtained by removing water and other volatile constituents from vegetation substances. In contrast to pollen, charcoal is more difficult to oxidize, even over relatively long time scale, e.g., the Miocene (Miao et al., 2016b). So, the taphonomic effect has little influence on either pollen or microcharcoals.

4.2.3 Effects of sedimentary processes

Sedimentary process can also affect the paleoclimatic record by sorting the pollen and microcharcoal assemblages. For example, different wind or fluvial velocities can sort and stratify the sedimentary grains differently: high velocities will blow or wash the fine grains away, leaving only the relative coarse grains to be buried. Dust particles and pollen/microcharcoal grains have similar sizes, if one particle type has been affected then it is likely that the other type will have been modified too. Here, we show the typical grain size changes of the dust particles to illustrate this issue (Figure 8).

Many exposures of loess sediments have yielded time series of particle size variations which are the basis for proxy climatic reconstructions (e.g., Ding et al., 2002; Fang et al., 2002). In the Ili Basin, the grain size distribution is dominated by silts (4-63 μm, mainly ~70%-84%), followed by a considerable percentage (10%-20%) of <4 μm clays fractions, and a minor proportion of 63-100 μm (2%-10%) and >100 μm (0-6%) sands fractions, respectively (Figure 8) (Yang et al., 2014). In the diagram, three phases bounded at ~1670 cm (47.5 ka) and ~780 cm (36 ka), can be identified. Due to the positive relationship between wind strength and grain size in the aeolian sediments (Xiao et al., 1995), the increase in coarse particle sizes may indicate an increase in wind strength (Ding et al., 2002; Fang et al., 2002). So, the two boundaries reflect marked changes in the wind strength. Within the 1670-500 cm range, there is a clear lack of significant variations in either the mean size (Figure 6) or the detailed grain-size distribution: the only relatively notable change occurs at ~1450 cm (45 ka ago) (Figure 9). Thus, no sedimentary processes driven by wind strength have influenced the dust particles, and therefore the wind has had little effect on either the pollen or the microcharcoals. Clay mineral records (illite, chlorite, kaolinite and smectite) from the same section (Li et al., 2017) have also been presented here for comparison. Regardless of their paleoclimate indications, obvious changes only occurred at 1450 cm (45 ka ago). No other anomalies occurred within the 1670-780 cm range (Figure 8). Therefore, the sedimentary process has also had little influence on the records of pollen and microcharcoals in the NLK section.

4.2.4 Human activities

If neither the climate changes across Central Asia nor the taphonomic/sedimentary processes have attributed to the climatic/ecologic variations and fire anomalies in the Ili Basin, alternative factors must be considered.

Besides climate change, fire is another factor causing changes to vegetation and land cover (Bird and Cali, 1998; Bowman et al., 2009; Miao et al., 2016a; Sirocko et al., 2016), which can subsequently lead to localized climatic anomalies. In Figure 7, we compiled the microcharcoal data to investigate the fire intensity on a relatively regional scale ($MC_{>50\ \mu m}/MC>_{50\ \mu m}$), including local forest fires ($MC_{R>50\ \mu m}/MC_{R>50\ \mu m}$) and local grass fires ($MC_{L>50\ \mu m}/MC_{L>50\ \mu m}$) as well as extreme local fire events ($MC_{>100\ \mu m}/MC_{<50\ \mu m}$), based on the different shapes and sizes (see section 4.1). The results revealed two obvious fire anomaly periods: one during 47.5-36 ka, when local and extreme-local fires were markedly more intense, followed by a sharp decrease to a normal level at 36 ka; the second was during 6-0 ka, again characterized by strong local and extreme-local fires.

In nature, wildfire has existed since the vegetation began to colonize the land (Glasspool et al., 2004). According to Holocene fire records from the Northeast Tibetan Plateau (Miao et al., 2017), as well as global records on orbital time scales (Bird and Cali, 1998; Luo et al., 2001), climate change might have strongly driven the fire changes through its influence on humidity. Summer precipitation during 41-36 ka was at its highest level of the past 70 ka (Rao et al., 2013), which will have impeded burning. Therefore, precipitation change was not the key factor in the observed fire anomalies. Another possibility is that the fire was caused by human activities. The earliest human-controlled fire can be traced back to at least 0.8 million years in Israel (Goren-Inbar et al., 2004) or 0.4-0.5 million years for *Homo erectus pekinensis* in China (Weiner et al., 1998), which means that the humans had widely colonized the globe during the latest period of the Pleistocene e.g., the last glacial period, bringing their skills of fire control. The Ili Basin, as one of the most important passageways from Africa to high-latitude Asia, e.g., Baikal Lake, may have been burned during their colonization, thus the natural vegetation could have been strongly affected, especially the arbors. Cupressaceae, as a sensitive woody species in the mid latitudes of Central Asia, grows slowly and once destroyed, recovers very slowly. This could explain why Cupressaceae disappeared so quickly fast following human colonization.

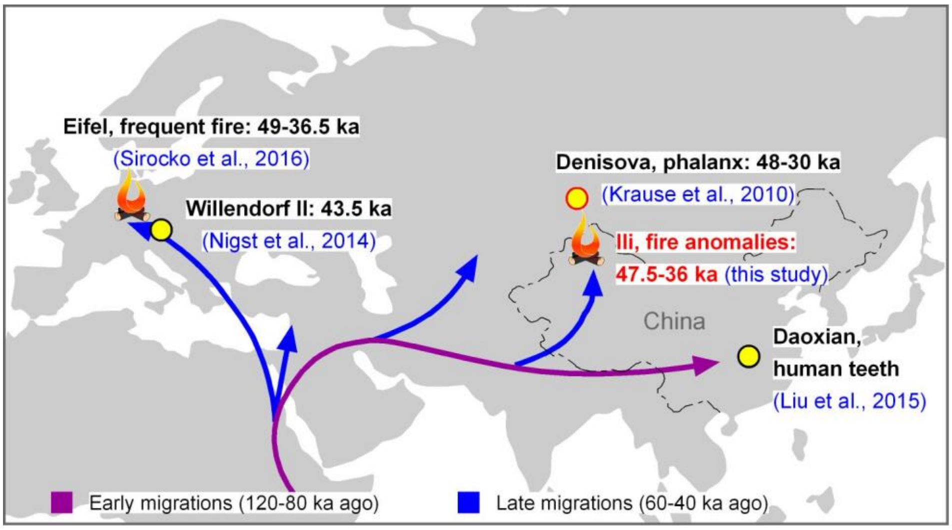

Figure 10. An early migration from Africa (adapted from Callaway, 2015). Fire anomalies found in the Ili Basin, Central Asia dated to 47.5-36 ka (this study) and frequent fires explained as the result of the natural forest in Europe dated to 49-36.5 ka (Sirocko et al., 2016) are plotted.

There is widespread evidence supporting human occupation of Central Asia during the Holocene (Huang et al., 1988; Wang and Zhang, 1988; Taklimakan Desert archaeology group, 1990; Yidilis, 1993; Lu et al., 2010; Zhang et al., 2011; Tang et al., 2013; Han et al., 2014). In the Ili Basin, although direct archeological sites are limited, the coeval local fire intensification supports human activity as a factor causing fire anomalies after ca.6 ka. This relationship can be similarly extended to observed fire anomalies at 47.5-36 ka, when humans migrated into the Ili Basin. Although direct archeological proofs of fire usage at this time are still lacking, human colonization of mid-to high-latitude Eurasia occurred after 200 to 80 ka (Liu et al., 2015) and extended to Central Asia after around 60-40 ka (Callaway, 2015): for example, Denisova Cave, in the Altai Mountains, Russia. The phalanx was found in a stratum dated to 48–30 ka ago (Krause et al., 2010) (Figures 8, 10). So, it is not difficult to link the local fire anomalies during 47.5-36 ka in the Ili Basin to human activities: the increased occurrence of local fires (for cooking, or burning the uncultivated land) quickly destroyed the vegetation, causing the observed vegetation degeneration. If this is the case, the modern vegetation characteristics may have merged at around 36 ka ago. In future, the use of a widespread and sustained ecological program of vegetation rehabilitation in the arid and semiarid region should reduce the risk of destructive fire, and will avoid a local vegetation disaster similar to that which occurred at 36 ka.

Interestingly, in Europe, the charcoal maxima show high frequent forest fires during 49-36.5 ka, explained as the result of the natural taiga fires under frequent drought stress. This is because the strongest fires at ~45 ka ago predate the movement of anatomically modern humans into central Europe (Sirocko et al., 2016). However, modern humans spreading into this area have been dated as early as ~43.5 ka (Nigst et al., 2014), very close to the fire maxima (Figure 9). Furthermore, according to the pollen assemblages in this study, there are two other periods (besides that during 49-36.5 ka) dominated by boreal forests, at around 147-105 ka and 15-10.5 ka, respectively (Sirocko et al., 2016). If a similar natural climate can play a similar dominant role in the vegetation and fire patterns, then the abundance of charcoal fragments during these two similar periods should be broadly higher, yet the values are almost the same as those of other periods dominated by other vegetation types (Sirocko et al., 2016). Therefore, the natural climate and forest changes may be not the key factors explaining the abnormal fire frequencies, and instead the human activities in Central Europe during 49-36.5 ka should not be discounted.

5. Conclusions

In the Ili Basin, pollen assemblages over the past 70 ka show a rapid vegetation change at ~36 ka characterized by increasing herbs and decreasing Cupressaceae, explained as the result of local fire intensification during 47.5-36 ago rather than particular taphonomic effects or sedimentary processes. Human activities may be inferred as one of the main driving forces of these anomalies, although no direct archeological proofs have been investigated. In future, archeological investigation in this area is required to check this hypothesis.

Acknowledgements

The project is supported by the Natural Science Foundation of China (Nos: 41572162, 41472147 and 41271215), the National Key Research and Development Program of China (Nos: 2016YFA0601902), International partnership Program of Chinese Academy of Science (grant number: 132B61KYS20160002), and the State Key Laboratory of Loess and Quaternary Geology, Institute of Earth Environment, CAS (SKLLQG1515) and Open Foundation of MOE Key Laboratory of Western China's Environmental System, Lanzhou University (lzujbky-2015- bt01). The authors thank Y. Li, X. Li, J. Dong and F. Zhang for sampling and laboratory assistance.

References

Ahn J, Brook EJ (2008) Atmospheric CO_2 and climate on millennial time scales during the last glacial period. Science, 322 (5898), 83-85.

Allen JRM, Brandt U, Brauer A et al (1999) Rapid environmental changes in southern Europe during the last glacial period. Nature 400, 740-743.

Andersen KK, Azuma N, Barnola JM et al (2004). High-resolution record of Northern Hemisphere climate extending into the last interglacial period. Nature, 431 (7005), 147-151.

Aranbarri J, González-Sampériz P, Valero-Garcés B, Moreno A, Gil-Romera G, Sevilla-Callejo M, García-Prieto E, Di Rita M., Mata P, Morellón M, Magri D, Rodríguez-Lázaro J, Carrión JS (2014). Rapid climatic changes and resilient vegetation during the Lateglacial and Holocene in a continental region of south-western Europe. Global and Planetary Change, 114, 50-65.

Augustin L, Barbante C, Barnes PR et al (2004) Eight glacial cycles from an Antarctic ice core. Nature, 429 (6992), 623-628.

Behling H, Safford HD (2010) Late-glacial and Holocene vegetation, climate and fire dynamics in the Serra dos Órgãos, Rio de Janeiro State, southeastern Brazil. Global Change Biology, 16 (6), 1661-1671.

Bird M, Cali J (1998) A million-year record of fire in sub-Saharan Africa. Nature, 394 (6695), 767-769.

Blunier T, Brook EJ (2001) Timing of millennial-scale climate change in Antarctica and Greenland during the last glacial period. Science, 291 (5501), 109-112.

Bond G, Showers W, Cheseby M et al (1997) A pervasive millennial-scale cycle in North Atlantic Holocene and glacial climates. Science 278, 1257-1266.

Bowman DM, Balch JK, Artaxo P et al (2009) Fire in the Earth system. science, 324 (5926), 481-484.

Callaway E (2015) Teeth from China reveal early human trek out of Africa-"Stunning" find shows that Homo sapiens reached Asia around 100,000 years ago. Nature News, (www.nature.com/news/teeth-from-china-reveal-early-human-trek-out-of-africa-1.18566)

Chen FH, Bloemendal J,Wang JM, Li JJ, Oldfield F (1997) High-resolution multiproxy climate records from Chinese loess: evidence for rapid climatic changes over the last 75 ka. Palaeogeography, Palaeoclimatology, Palaeoecology 130, 323-335.

Chen FH, Cheng B, Zhao Y, et al. (2006) Holocene environmental change inferred from a high-resolution pollen record, Lake Zhuyeze, arid China. The Holocene, 16 (5), 675-684.

Cheng H, Zhang PZ, Spötl C et al (2012) The climatic cyclicity in semiarid-arid central Asia over the past 500,000 years. Geophysical Research Letters, 39 (1), L0170510.

Clark JS (1988) Particle motion and the theory of charcoal analysis: source area, transport, deposition, and sampling. Quaternary Research, 30 (1), 67-80.

Clark JD, Harris JWK (1985) Fire and its roles in early hominid lifeways. Afr Archaeol Rev 3:3–27.

Conard NJ, Bolus M (2008). Radiocarbon dating the late Middle Paleolithic and the Aurignacian of the Swabian Jura. J. Hum. Evol. 55 (5), 886-897.

Conard NJ, Bolus M, Goldberg P, et al (2006) The last Neanderthals and firstmodern humans in the Swabian Jura. When Neanderthals and Modern Human Met. Tübingen Publications in Prehistory, Kerns Verlag, Tübingen, pp. 305-342.

Crawford AJ, Belcher CM (2014) Charcoal morphometry for paleoecological analysis: The effects of fuel type and transportation on morphological parameters. Applications in plant sciences, 2, 8.

Derevianko AP, Petrin VT, Rybin EP (2000). The Kara-Bom site and the characteristics of the Middle to Upper Palaeolithic transition in the Altai. Archaeol. Ethnol. Anthropol. Eurasia 2, 33-52.

Ding ZL, Derbyshire E, Yang SL et al (2002) Stacked 2.6-Ma grain size record from the Chinese loess based on five sections and correlation with the deep-sea delta O-18 record. Paleoceanography 17.

Gowlett, J. A. J. Wrangham, R (2013). Earliest fire in Africa: towards the convergence of archaeological evidence and the cooking hypothesis. Azania:. Archaeol. Res. Afr. 48 (1), 5-30.

Fang XM, Shi ZT, Yang SL, et al (2002) Loess in the Tian Shan and its implications for the development of the Gurbantunggut Desert and drying of northern Xinjiang. Chin. Sci. Bull. 47, 1381-1387.

Filion L (1984) A relationship between dunes, fire and climate recorded in the Holocene deposits of Quebec. Nature, 543-546.

Glasspool IJ, Edwards D, Axe L (2004) Charcoal in the Silurian as evidence for the earliest wildfire. Geology, 32 (5), 381-383.

Goebel T, Derevianko AP, Petrin VT (1993) Dating the Middle-to-Upper- Paleolithic Transition at Kara-Bom. Curr. Anthropol. 34, 452-458.

Goren-Inbar N, Alperson N, Kislev ME et al (2004) Evidence of hominin control of fire at Gesher Benot Yaaqov, Israel. Science, 304 (5671), 725-727.

Guiot J, De Beaulieu JL, Cheddadi R et al (1993) The climate in Western Europe during the last Glacial/Interglacial cycle derived from pollen and insect remains. Palaeogeography, Palaeoclimatology, Palaeoecology 103 (1), 73-93.

Guo ZT, Liu TS, Guiot J et al (1996) High frequency pulses of East Asian monsoon climate in the last two glaciations: link with the North Atlantic. Climate Dynamics, 12 (10), 701-709.

Han WX, Lu LP, Lai Z, Madsen D, Yang SL (2014) The earliest well-dated archeological site in the hyper-arid Tarim Basin and its implications for prehistoric human migration and climatic change. Quaternary Research, 82 (1), 66-72.

Hao Q, Wang L, Oldfield F et al (2012) Delayed build-up of Arctic ice sheets during 400,000-year minima in insolation variability. Nature, 490, 7420, 393-396.

Huang CC, Pang J, Chen S et al (2006) Charcoal records of fire history in the Holocene loess-soil sequences over the southern Loess Plateau of China. Palaeogeography, Palaeoclimatology, Palaeoecology, 239, 1, 28-44.

Huang WW, Olsen JW, Reevesx RW, Miller-Antonio S, Lei JQ (1988) New discoveries of stone artifacts on the southern edge of the Tarim Basin, Xinjiang. Acta Anthropologica Sinica 4, 294-301 (in Chinese).

Hubau W, Van den Bulcke J, Van Acker J, Beeckman H (2015) Charcoal-inferred Holocene fire and vegetation history linked to drought periods in the Democratic Republic of Congo. Global change biology, 21(6), 2296-2308.

Jiang HC, Mao X, Xu H, Thompson J, Wang P, Ma X (2011) Last glacial pollen record from Lanzhou (Northwestern China) and possible forcing mechanisms for the MIS 3 climate change in Middle to East Asia. Quaternary Science Reviews, 30 (5), 769-781.

Krause J, Fu Q, Good JM, Viola B, Shunkov MV, Derevianko AP, Pääbo S (2010). The complete mitochondrial DNA genome of an unknown hominin from southern Siberia. Nature, 464 (7290), 894-897.Krause J, Orlando L, Serre D, et al. (2007) Neanderthals in central Asia and

Siberia. Nature 449, 902-904.

Li XZ, Liu XD, Qiu LJ, An ZS, Yin ZY (2013) Transient Simulation of Orbital-scale Precipitation Variation in Monsoonal East Asia and Arid Central Asia during the Last 150 ka. J. Geophys. Res., 118, 7481-7488.

Li Y, Song Y, Lai Z, Han L, An Z (2016) Rapid and cyclic dust accumulation during MIS 2 in Central Asia inferred from loess OSL dating and grain-size analysis. Scientific Reports, 6, e32365, 32361-32366.

Li Y, Song YG, Yan LB, Chen T, An ZS (2015) Timing and Spatial Distribution of Loess in Xinjiang, NW China. Plos One, 10, 5.

Li Y, Song YG, Zeng MX, et al. (2017) Tiliwaldi Halmurat6Evaluating paleoclimatic significance of clay mineral records from a late-Pleistocene loess-paleosol section of the Ili Basin, Central Asia. Quaternary Research (accepted).

Liu W, Martinón-Torres M, Cai YJ et al (2015) The earliest unequivocally modern humans in southern China. Nature doi:10.1038/nature15696

Lu HY, Xia XC, Liu JQ et al (2010) A preliminary study of chronology for a newly discovered ancient city and five archaeological sites in Lop Nur, China. Chin Sci Bull 55 (1), 63-71 (in Chinese).

Luo Y, Chen H, Wu G, Sun X (2001) Records of natural fire and climate history during the last three glacial-interglacial cycles around the South China Sea. Science in China Series D: Earth Sciences, 44, 10, 897-904.

Maher LJ (1981) Statistics for microfossil concentration measurements employing samples spiked with marker grains. Review of Palaeobotany and Palynology, 32(2-3), 153-191.

Miao YF, Jin H, Cui J (2016a) Human activity accelerating the rapid desertification of the Mu Us Sandy Lands, North China. Scientific reports, 6.

Miao YF, Fang XM, Song CH, et al. (2016b) Late Cenozoic fire enhancement response to aridification in mid-latitude Asia: Evidence from microcharcoal records. Quaternary Science Reviews, 139, 53-66.

Miao YF, Zhang D, Cai X et al (2017) Holocene fire on the northeast Tibetan Plateau in relation to climate change and human activity. Quaternary International, 443, 124-131

Nigst P R, Haesaerts P, Damblon F, et al. (2014). Early modern human settlement of Europe north of the Alps occurred 43,500 years ago in a cold steppe-type environment. Proceedings of the National Academy of Sciences 111(40), 14394-14399.

Patterson WA, Edwards KJ, Maguire DJ (1987) Microscopic charcoal as a fossil indicator of fire. Quaternary Science Reviews, 6 (1), 3-23.

Petit JR, Jouzel J, Raynaud D et al (1999) Climate and atmospheric history of the past 420,000 years from the Vostok ice core, Antarctica. Nature, 399 (6735), 429-436.

Porter SC, An ZS (1995) Correlation between climate events in the North Atlantic and China during the last glaciation. Nature 375, 305- 308.

Rao ZG, Chen FH, Cheng H et al (2013) High-resolution summer precipitation variations in the western Chinese Loess Plateau during the last glacial. Scientific reports, 3, 2785.

Sirocko F, Knapp H, Dreher F, Förster MW, Albert J, Brunck H, Röhner M, Rudert S, Schwibus K, Adams C, Sigl P (2016). The ELSA-Vegetation-Stack: Reconstruction of Landscape Evolution Zones (LEZ) from laminated Eifel maar sediments of the last 60,000 years. Global and Planetary Change, 142, 108-135.

Song YG, Chen XL, Qian LB et al (2014) Distribution and composition of loess sediments in the Ili Basin, Central Asia. Quaternary International 334-335, 61-73.

Song YG, Lai ZP, Li Y et al (2015) Comparison between luminescence and radiocarbon dating of late Quaternary loess from the Ili Basin in Central Asia. Quaternary Geochronology, 30, 405-410.

Song YG, Shi ZT, Fang XM et al (2010) Loess magnetic properties in the Ili Basin and their correlation with the Chinese Loess Plateau. Science China Earth Sciences 53, 419-431.

Sun YB, Clemens SC, Morrill C et al (2012) Influence of Atlantic meridional overturning circulation on the East Asian winter monsoon. Nature Geosci, 5 (1), 46-49.

Taklimakan Desert archaeology group (1990) Microlithic in the AltunMountains. Xinjiang Cultural Relics 4, 14-18 (in Chinese)

Tang ZH, Chen D, Wu X, Mu G. (2013) Redistribution of prehistoric Tarim people in response to climate change. Quat Int 308, 36-41.

Templeton A (2002) Out of Africa again and again. Nature, 416 (6876), 45-51.

Thompson L, Yao TD, Davis M et al (1997) Tropical climate instability: The last glacial cycle from a Qinghai-Tibetan ice core. Science, 276 (5320), 1821-1825.

Umbanhowar CE, Mcgrath MJ (1998) Experimental production and analysis of microscopic charcoal from wood, leaves and grasses. The Holocene, 8 (3), 341-346.

Varela S, Lima-Ribeiro MS, Diniz-Filho JAF, Storch D (2015) Differential effects of temperature change and human impact on European Late Quaternary mammalian extinctions. Global change biology, 21 (4), 1475-1481.

Wang B, Zhang TN (1988) New discoveries of the Paleolithic archaeology in Xinjiang. Social Science Research of Xinjiang 11, 35-36 (in Chinese).

Wang QS., Song YG, Zhao ZJ, Li JJ (2016) Color characteristics of Chinese loess and its paleoclimatic significance during the last glacial-interglacial cycle. J Asian Earth Sci 116, 132-138.

Wang X, Xiao J, Cui L, Ding ZL (2013) Holocene changes in fire frequency in the Daihai Lake region (north-central China): indications and implications for an important role of human activity. Quaternary Science Reviews, 59, 18-29.

Wang YJ, Cheng H, Edwards RL, et al (2001). A high-resolution absolute-dated late Pleistocene monsoon record from Hulu Cave, China. Science, 294 (5550), 2345-2348

Weiner S, Xu Q, Goldberg P, Liu J, Bar-Yosef O (1998) Evidence for the use of fire at Zhoukoudian, China. Science, 281, 251-253.

Whitlock C, Larsen C (2002) Charcoal as a fire proxy, Tracking environmental change using lake sediments, Springer, 75-97.

Wu FL, Fang XM, Ma YZ, et al. (2007) Plio–Quaternary stepwise drying of Asia: Evidence from a 3-Ma pollen record from the Chinese Loess Plateau. Earth and Planetary Science Letters, 257 (1), 160-169.

Xiao JL, Porter SC, An ZS, Kumai H, Yoshikawa S (1995) Grain-Size of Quartz as an Indicator of Winter Monsoon Strength on the Loess Plateau of Central China during the Last 130,000-Yr. Quaternary Research 43, 22-29.

Yang SL, Forman SL, Song YG et al (2014) Evaluating OSL-SAR protocols for dating quartz grains from the loess in Ili Basin, Central Asia. Quat Geoch 20, 78-88.

Ye BH, Lai ZM, Shi YF (1997) Some characteristics of precipitation and air temperature in the Yili River Basin (in Chinese). Arid Land Geogr. 20, 47-52.

Ye W (2001) Sedimentary Characteristics of Loess and Paleoclimate in Westerly Region of

Xinjiang. China Ocean Press, Beijing, p. 179 (in Chinese with English abstract).

Yidilis A (1993) Microlithic sites in Xinjiang. Xinjiang Cultural Relics 4, 17-18 (in Chinese).

Zhang F, Wang T, Yimit H et al (2011) Hydrological changes and settlement migrations in the Keriya River delta in central Tarim Basin ca. 2.7-1.6 ka BP: inferred from14C and OSL chronology. Sci China Earth Sci 41, 1495-1504 (in Chinese).

Zhao Y, Chen F, Zhou A, Yu Z, Zhang K (2010) Vegetation history, climate change and human activities over the last 6200years on the Liupan Mountains in the southwestern Loess Plateau in central China. Palaeogeography, Palaeoclimatology, Palaeoecology, 293 (1), 197-205.